The utility of contrast-enhanced FDG-PET/CT in the clinical management of pancreatic cancer: Impact on diagnosis, staging, evaluation of treatment response, and detection of recurrence

Running title: Contrast-enhanced PET/CT in pancreatic cancer

Akinori Asagi, MD[1]; Koji Ohta, PhD[2]; Junichirou Nasu, MD, PhD[1]; Minoru Tanada, MD[2]; Seijin Nadano, MD[1]; Rieko Nishimura, MD, PhD[3]; Norihiro Teramoto, MD, PhD[3]; Kazuhide Yamamoto, MD, PhD[5]; Takeshi Inoue, MD, PhD[4]; Haruo Iguchi, MD, PhD[1]

Departments of [1]Gastroenterology, [2]Gastroenterological Surgery, [3]Pathology, and [4]Diagnostic Radiology, Shikoku Cancer Center, and [5]Department of Gastroenterology and Hepatology, Okayama University Graduate School of Medicine

Corresponding author:
Haruo Iguchi
Department of Gastroenterology, Shikoku Cancer Center
Minami-Umemotomachi Ko 160, Matsuyama, Ehime 791-0280, Japan.
Tel: +81-89-999-1111, Fax: +81-89-999-1128
E-mail: higuchi@shikoku-cc.go.jp

Acknowledgments

This work was supported in part by a Grant-in-Aid for Research on Applying Health Technology (Grant No. H23-Cancer-General-010) from the Ministry of Health, Labor, and Welfare of Japan and Management Expenses Grants (Grant No. 22-54) from the Japanese government to the National Cancer Center.

Abstract

Objectives: Fluorodeoxyglucose(FDG)-positron emission tomography/contrast enhanced-computed tomography (PET/CE-CT) involving whole-body scanning first by non-CE-CT and FDG-PET, followed by CE-CT has been used for detailed examination of pancreatic lesions. We evaluated PET/CE-CT images with regard to differential diagnosis, staging, treatment response, and postoperative recurrence in pancreatic cancer.

Methods: PET/CE-CT was conducted in 108 patients with pancreatic cancer and 41 patients with other pancreatic tumor diseases.

Results: The maximum standardized uptake value (SUV_{max}) overlapped in benign and malignant cases, suggesting that differential diagnosis of pancreatic tumors based on the SUV_{max} is difficult. In the evaluation of staging in 31 resectable pancreatic cancer by PET/CE-CT, the diagnostic accuracy rate was more than 80% for most factors concerning local invasion and 94% for distant metastasis, but only 42% for lymph node metastasis. Significant positive correlations were found between the SUV_{max} and tumor size/markers, suggesting that SUV_{max} may be a useful indicator for the treatment response. Regarding the diagnosis of the postoperative recurrence, PET/CE-CT correctly detected local recurrence in all the 11 cases of recurrence, while abdominal CE-CT detected only 7 out of 11 cases, suggesting that PET/CE-CT is superior in this context.

Conclusions: PET/CE-CT is useful for the clinical management of pancreatic cancer.

Keywords: contrast-enhanced PET/CT (PET/CE-CT), differential diagnosis, clinical management, pancreatic cancer

Introduction

Despite recent significant advances in cancer diagnosis and treatment, pancreatic cancer patients still have a very poor prognosis [1]. In Japan, the number of pancreatic cancer patients in 2002 was 21,386, while the number of pancreatic cancer-related deaths in 2006 was 23,366 [2], indicating that the number of patients with pancreatic cancer was almost equal to the number of pancreatic cancer-related deaths. However, a slight improvement in survival has been observed with the introduction of gemcitabine (GEM) and S-1 as chemotherapeutic medications for pancreatic cancer [3, 4]. Given this situation, clinical practice guidelines for pancreatic cancer have recently been established in Japan, and treatment regimens are determined on the basis of the extent of pancreatic cancer, which is evaluated by imaging. Contrast-enhanced-abdominal CT (abdominal CE-CT) has primarily been used to determine the extent of pancreatic cancer [5]. However, imaging diagnosis is also essential in the postoperative monitoring of pancreatic cancers, which often recur soon after surgery; abdominal CE-CT imaging has also been used for this purpose.

Positron emission tomography (PET), a new imaging modality, has recently been introduced in daily clinical practice, but functional imaging by PET alone does not have much diagnostic significance [6]. Acquisition of consecutive PET and CT (PET/CT) images in addition to combination of functional PET and anatomical CT images dramatically enhances the usefulness of PET as an imaging modality [7]. We have been using PET/CT (Aquiduo16; Toshiba) since the introduction of this technique at the Shikoku Cancer Center in April 2006; the CT apparatus has been dedicated to dynamic studies (contrast-enhanced PET/CT [PET/CE-CT]) on the development of this technique as a key imaging modality in the diagnosis and follow-up examinations of patients with pancreatic cancer. In this study, we retrospectively compared

PET/CE-CT and abdominal CE-CT, which has been used as the primary imaging modality for the diagnosis and management of pancreatic cancer, and evaluated the efficacy of these modalities for the following functions: differential diagnosis of benign and malignant pancreatic lesions, evaluation of the extent of invasive pancreatic ductal cancer, assessment of treatment effects, and diagnosis of postoperative recurrence.

Material and Methods

Subjects

PET/CE-CT imaging technology was used to determine the extent of invasive pancreatic ductal cancer in 108 patients (64 men and 44 women, ages 45–86 years). The extent of cancer was determined according to Classification of Pancreatic Carcinoma 5th Edition (edited by the Japan Pancreas Society) [8]. Among the 108 subjects, operations were performed on 29 patients with locally advanced pancreatic ductal cancer, and the histological diagnosis was proven in these patients. The remaining patients were diagnosed on the basis of PET/CE-CT imaging findings and serum tumor marker values.

PET/CE-CT imaging was conducted for relevant pancreatic tumor lesions to assess the usefulness of the maximum standardized uptake value (SUV_{max}) in differentiating benign and malignant pancreatic lesions. The SUV_{max} was the value obtained at 90 min after intravenous injection of fluorodeoxyglucose (FDG) in subjects with blood glucose levels of 200 mg/dL or less at the time of FDG administration.

Differential diagnosis for malignant and benign pancreatic disorders by PET/CE-CT imaging was performed in 21 patients with intraductal papillary mucinous neoplasm (IPMN; 9 men and 12 women; age, 47–78 years), 10 patients with endocrine tumors of the pancreas (2 men and 8

women; age, 42–78 years), and 10 patients with tumor-forming pancreatitis (chronic pancreatitis [CP] or autoimmune pancreatitis [AIP]; 8 men and 2 women; age, 40–79 years) in addition to the 108 patients with invasive pancreatic ductal cancer. Among the 21 IPMN patients, 8 patients underwent operations, and the diagnosis of malignant tumors (intraductal papillary mucinous carcinoma [IPMC]) and benign tumors (intraductal papillary mucinous adenoma [IPMA]) was histologically proven in these patients. The remaining 13 patients were diagnosed with benign tumors (IPMA) based on the findings from imaging studies (PET/CE-CT, MRI, US), including branch type, lack of internal structures, and lack of FDG uptake. These patients are currently being observed by follow-up at more than 1 year after diagnosis. Ten patients with endocrine tumors of the pancreas were diagnosed based on the presence of hypervascular tumors with FDG accumulation upon PET/CE-CT imaging. Among these patients, 7 underwent operations, and biopsies were performed in the remaining 3 patients, resulting in histologically proven diagnoses for all 10 patients. Malignancy and benignancy were determined based on histological findings and by taking into account the presence or absence of metastatic lesions on the images. Chronic pancreatitis and AIP were diagnosed by PET/CE-CT imaging and serum levels of pancreatic enzymes and/or IgG4 according to the Diagnostic Criteria for Chronic Pancreatitis 2002 [9] and the Diagnostic Criteria for Autoimmune Pancreatitis 2006 (Japan Pancreas Society) [10].

Classification of pancreatic cancer

In this study, we employed the classification system for pancreatic cancer defined by the Japan Pancreas Society (JPS) [8]. According to the JPS classification system, the extent of invasive pancreatic ductal cancer was determined by taking into account local spread (T), lymph node

metastases (N), and distant metastases (M). The T category was defined through determination of the presence and extent of local invasion of the pancreas and adjacent structures. Within this category, 8 local extension factors were considered: the distal bile duct (CH), duodenum (DU), serosa (S), retropancreatic tissue (RP), portal venous system (PV), arterial system (A), extrapancreatic nerve plexus (PL), and other organs (OO). The N category (lymph node metastases) was divided into 4 categories (N0–N3) according to whether metastasis was present in lymph nodes with groups 1–3. The presence of distant metastatic lesions, including metastasis to distant organs, the peritoneum, and group 3 lymph nodes, were defined as M1. Based on the grading for T, N, and M categories, tumor stage was divided into 5 groups, as shown in Fig. 1. A detailed description of stage grouping by JPS guidelines is described in a previous report by Isaji et al. [8].

PET/CT imaging protocol

All FDG-PET/CT studies were performed using an Aquiduo PET/CT scanner (Toshiba, Otawara, Japan), which is a hybrid PET and 16-MDCT scanner. Patients fasted for at least 4 h before the PET/CT examination. In all patients, blood glucose levels were checked before injection of the radiopharmaceutical. Intravenous injection of 3.0 MBq/kg body weight of FDG was followed by a 10-mL normal saline flush. Patients rested for about 90 min, during which time they were asked to drink 500 mL of a Japanese tea containing 5 mL of oral contrast media (Gastrografin; Bayer Schering Pharma) prior to image acquisition and to void before being positioned supine on the scanner table. Noncontrast CT was performed first, from the vertex of the skull through the mid thigh at 80–200 mAs, 120 kVp, and 2.0-mm collimation. Images were reconstructed as contiguous 4-mm slices. PET was performed immediately after noncontrast CT without

repositioning the patient. PET images were obtained at 7–8 stations per patient, with an acquisition time of 2–3 min per station, from the skull vertex through the mid thigh. The noncontrast CT data were used for attenuation correction of PET emission images, which were coregistered with the noncontrast CT dataset. Then, dual phase contrast-enhanced CT was performed. Arterial phase CT images were obtained 35 sec after injection of 100 mL iopamidol (Iopamiron 300, Bayer Schering Pharma). Contrast material was injected at 3 mL/s using a powder injector (Dual Shot GV, Nemoto). Arterial phase images were obtained from the dome of the diaphragm to the iliac crest at 80–200 mAs, 120 kVp, and 1.0-mm collimation. Arterial phase images were reconstructed as contiguous 2-mm slices. Portal venous phase images were acquired after a delay of 90 sec from the vertex of the skull through the mid thigh at 80–200 mAs, 120 kVp, and 2.0-mm collimation. Portal venous phase images were reconstructed as contiguous 2-mm slices.

PET/CT imaging using this protocol (PET/CE-CT) can cover all angles of the diagnosis, including diagnosis of existing tumors, qualitative diagnosis, local diagnosis, and metastasis detection.

Evaluation of the extent of invasive pancreatic ductal cancer

Operations were performed on 29 patients with locally advanced pancreatic ductal cancer (Stage IVa), and diagnoses were histologically proven in these patients. Postoperatively, findings from PET/CE-CT imaging of the pre-operative cancer were compared with the histological findings of the resected specimens in order to determine the diagnostic accuracy rate of PET/CE-CT imaging for the evaluation of the extent of cancer progression. The degree of pre-operative and postoperative cancer progression was determined according to the JPS

classification system [8]. In another 4 patients with invasive pancreatic ductal cancer, whose pre-operative stage was diagnosed as resectable IVa by PET/CE-CT, only metastatic tissue biopsies were performed since distant metastases were found after initiation of the surgical procedure (lymph node [N3], 2 cases; liver, 1 case; peritoneum, 1 case). Thus, N and M categories were examined in 31 patients with stage IVa after the addition of these 2 cases. We also compared the diagnostic accuracy rate of PET/CE-CT imaging with that of abdominal CE-CT imaging, which was extracted from the PET/CE-CT imaging, for evaluating cancer extent.

We further evaluated the diagnostic accuracy rate of PET/CE-CT for M factor analysis in 65 patients with stage IVb unresectable pancreatic cancer, since distant metastases are not normally found in stage IVa resectable pancreatic cancer, and compared it with that of CE-CT images, which were extracted from the PET/CE-CT images. In this analysis, the reference standard for the presence of distant metastases was based on multimodality images and follow-up observations since distant metastases were not histologically proven.

To compare the diagnostic accuracy rates of PET/CE-CT and abdominal CE-CT in the context of evaluating T, N, and M factors, 2 radiologists were asked to analyze sections from these images independently, without knowledge of the results of the other imaging. If a disagreement occurred, a final decision was made after a discussion of the radiologists' analyses.

Assessment of treatment effects

The effects of treatment were evaluated over time in 8 patients who had undergone chemotherapy or chemoradiotherapy for unresectable locally advanced pancreatic cancer, diagnosed using PET/CE-CT imaging (tumor diameter determined by CT and SUV_{max} determined by PET) and serum tumor marker levels (CA19-9). After determining the rate of increases and

decreases in tumor diameter, SUV_{max} values and CA19-9 levels were assessed, and correlations among these factors were examined. This analysis was conducted only on patients whose pancreatic cancer was locally confined during the ongoing treatment and was discontinued whenever distant metastasis occurred. At each evaluation of treatment effectiveness, the change rate of each variable was calculated and examined for correlations. Therefore, although 8 patients were analyzed, the number of analyzable events was 12, since multiple events occurred per case.

Diagnosis of postoperative recurrence

While pancreatic cancer often recurs soon after surgery, the anatomical positional relationship between various abdominal organs may be changed by surgery; therefore, an abdominal CE-CT scan alone is often insufficient for diagnosis of local recurrence, not to mention distant metastasis. In the present study, PET/CE-CT images were used to show postoperative recurrence in 11 patients and a lack of postoperative recurrence of invasive pancreatic ductal cancer in 6 patients. Local recurrence was diagnosed by PET/CE-CT based on the findings of soft tissue-density mass with FDG accumulation, while soft tissue-density mass without FDG accumulation was diagnosed as a postoperative change. The diagnosis of local recurrence by abdominal CE-CT, on the other hand, requires not only the presence of soft tissue-density mass, but also the ability to compare the mass with the size with the previously measured mass. Thus, an increase in the size of the soft tissue-density mass was considered a local recurrence, while no increase and/or little increase in size was considered a lack of local recurrence. However, there is no standard criteria defining the increase in size that would constitute a local recurrence; thus, the diagnosis of local recurrence depends on the radiologist. In our cancer center, PET/CE-CT is usually conducted on patients in whom the serum levels of tumor markers are elevated during the follow-up period. To

determine the diagnostic accuracy rate of abdominal CE-CT for the evaluation of local recurrence, 2 radiologists were asked to read only sections from abdominal CE-CT scans extracted from PET/CE-CT imaging independently, without knowledge of the results of other imaging findings. If a disagreement occurred, a final decision was made after discussion between the radiologists. Then, the diagnostic accuracy rate for local recurrence was compared between PET/CE-CT and abdominal CE-CT imaging. Although local recurrences were not histologically proven, they were confirmed by follow-up observations after the initial diagnosis by PET/CE-CT. As a result, the diagnostic accuracy rate of PET/CE-CT was 100%.

Statistical analysis

Differences between the SUV_{max} values in various pancreatic disorders with tumorous lesions were evaluated using the *t*-test. Differences in the diagnostic accuracy rates of the tested imaging modalities (PET/CE-CT and abdominal CE-CT) were evaluated using the Cochran Q test. Relationships between changes in tumor size, SUV_{max} values, and serum CA-19-9 levels during treatment were evaluated using linear regression analysis. A *p*-value of less than 0.05 was considered statistically significant.

Results

1. Differential diagnosis of the malignancy and benignancy of pancreatic lesions by PET/CE-CT imaging

Fig. 2 shows the SUV_{max} of various pancreatic tumor diseases. The SUV_{max} (mean ± SD) of invasive pancreatic ductal cancer was 6.14 ± 3.51 in stages I–III, 6.28 ± 2.91 in stage IVa, and 7.22 ± 2.65 in stage IVb; thus, the values for different stages were not significantly different.

However, the SUV_{max} of invasive pancreatic ductal cancer tended to be higher than those of other pancreatic tumor diseases, excluding benign pancreatic endocrine tumors. In the case of IPMN, the SUV_{max} values (mean ± SD) were 3.09 ± 1.53 for IPMC (n = 5) and 1.59 ± 0.52 for IPMA (n = 16). The SUV_{max} of IPMC was significantly higher than that of IPMA ($P < 0.005$). In the case of pancreatic endocrine tumors, the SUV_{max} values (mean ± SD) were 27.4 ± 18.2 (n = 3) in benign cases and 4.21 ± 2.56 (n = 7) in malignant cases; thus, the SUV_{was} markedly higher in benign cases. Among 3 cases of benign endocrine tumors, 2 cases exhibited extremely high SUV_{max} values, 33.5 and 46.1, and the histological diagnosis for these cases was well-differentiated endocrine tumors with uncertain behavior according to the WHO classification of endocrine tumors published in 2004 [11]. These 2 cases have been followed up for more than 3 years, and recurrence was not noted until August 2011. In tumor-forming chronic pancreatitis and tumor-forming AIP, SUV_{max} values (mean ± SD) were 2.19 ± 0.48 (n = 5) and 4.76 ± 1.64 (n = 5), respectively; therefore, the SUV_{max} of AIP was significantly higher than that of chronic pancreatitis ($P < 0.01$).

2. Diagnostic accuracy rate of PET/CE-CT imaging for determining the extent of invasive pancreatic ductal cancer

The diagnostic accuracy rate of PET/CE-CT for T, N, and M factor in patients with stage IVa resectable pancreatic cancer is shown in Table 1.

With respect to the T factor, the diagnostic accuracy rate of PET/CE-CT imaging for tumor size (Ts), serosa(S), and retropancreatic tissue(RP) was below 80%, while it was greater than 80% for distal bile duct(CH), duodenum(DU), portal vein system(PV), arterial system(A), extrapancreatic nerve plexus(PL) and other organ(OO). Among these factors in the T category, A, PV, and PL are

important to determine whether the locally advanced pancreatic cancer (stage IVa) is resectable. The diagnostic accuracy rates of A, PV, and PL were 97%, 86%, and 83%, respectively. Evaluation of the T factor by PET/CE-CT was based on the findings of the CE-CT images; therefore, the diagnostic accuracy rate of PET/CE-CT for the T factor was identical to that of abdominal CE-CT (data not shown).

Abdominal CE-CT imaging was used to determine the extent of N factor based on the shape and size of lymph nodes, while FDG uptake was used as an additional evaluation element in PET/CE-CT imaging (Fig. 3). The accuracy rate of PET/CE-CT for the N factor was 42% (Table 1-A), while that of abdominal CE-CT was 35% in 31 patients with stage IVa resectable pancreatic cancer (data not shown). The breakdown of differentially diagnosed N factor characteristics as measured by PET/CE-CT and histological examination (n = 18) is shown in Table 1-B. Among these N factor diagnoses, overestimation and underestimation of the extent of N factor characteristics by PET/CE-CT were observed in 6 and 12 patients, respectively. In the 6 cases of overestimation, 4 were determined to be stage IVb unresectable cases solely based on the pre-operative evaluation of N2 or N3 by PET/CE-CT. In the 12 cases of underestimation, on the other hand, 9 with peripancreatic lymph node metastasis in the resected specimen, which is histologically diagnosed as N1, were included.

With respect to the M factor, the diagnostic accuracy rate of PET/CE-CT imaging was 94% in 31 patients with stage IVa resectable pancreatic cancer (Table 1-A). Two metastatic cases, 1 with metastasis to the surface of the liver and the other with miliary nodules of peritoneal dissemination, were not detected by the pre-operative PET/CE-CT. We also evaluated the diagnostic accuracy rate of PET/CE-CT for M factor characteristics in 65 patients with stage IVb unresectable pancreatic cancer (Table 2). Lymph node metastasis (N3), hepatic metastasis, and peritoneal

dissemination, which are often observed as distant metastasis of pancreatic cancer, were detected in 51%, 55%, and 53% of patients by PET/CE-CT and 45%, 53%, and 31% of cases by abdominal CE-CT, respectively. The detection rates of abdominal CE-CT for lymph node metastasis (N3) and peritoneal dissemination were significantly lower than that of PET/CE-CT, although the detection rate of hepatic metastasis was similar between the 2 methods. Lung and bone metastasis have rarely been detected by abdominal CE-CT because this type of imaging scans only a segmental area. PET/CE-CT imaging, on the other hand, scans the whole body, resulting in higher detection rates of lung and bone metastases (Table 2).

3. Assessment of treatment effects by PET/CE-CT imaging

Unresectable pancreatic cancer is treated with chemotherapy or chemoradiotherapy, and the effectiveness of treatment is assessed according to RECIST guidelines [12] by determining the longest diameter of the measurable lesion, which is usually measured using abdominal CE-CT, and levels of serum tumor marker.

We determined the increase/decrease ratios of tumor size, CA19-9 levels, and SUV_{max} in the progressive disease (PD) and partial response (PR) groups. In contrast to small changes in tumor size, the changes in CA19-9 levels and SUV_{max} values were larger, and the patterns of changes in these indicators were similar (Fig. 4-a). Among these 3 indicators, a significant positive correlation was found between SUV_{max} and CA19-9 levels ($P < 0.0001$) and between SUV_{max} and tumor size ($P < 0.05$), but no significant correlation was found between CA19-9 levels and tumor size (Fig. 4-b).

4. Diagnosis of postoperative recurrence

In patients with pancreatic cancer, recurrence is frequently observed shortly after the operation [13]; thus, diagnosis of recurrence is crucial for starting an appropriate treatment. Abdominal CE-CT is generally used for this diagnosis; however, in some cases, local recurrence may be difficult to detect because of postoperative alterations in the anatomical positions of visceral organs [14, 15]. Therefore, we compared the rates of postoperative local recurrences diagnosed by abdominal CE-CT and PET/CE-CT imaging. Abdominal CE-CT detected 7 out of the 11 cases diagnosed by PET/CE-CT imaging, and in 6 cases diagnosed as not having local recurrence by PET/CE-CT imaging, 5 cases were diagnosed correctly by abdominal CE-CT (Table 3). Typical findings from imaging of local recurrences by PET/CE-CT are shown in Fig. 5.

Discussion

Pre-operative evaluation of the extent of pancreatic cancer is important in deciding treatment options, and abdominal CE-CT is usually used for this purpose. In the present study, we determined the diagnostic accuracy rate of PET/CE-CT in evaluating the extent of pancreatic cancer, and compared it to that of abdominal CE-CT. The accuracy rate for diagnosing the T factor, which includes an evaluation of local spread or invasion into the area surrounding the pancreas, was less than 80% for tumor size(Ts), serosa(S), and retropancreatic tissue(RP), and greater than 80% for the distal bile duct(CH), duodenum(DU), portal vein system(PV), arterial system(A), extrapancreatic nerve plexus(PL) and other organ(OO). Among these factors, PV, A, and PL are important in deciding whether the tumors are resectable or not, and the accuracy rates of PET/CE-CT for these factors (PV, 86%; A, 97%; and PL, 87%) were satisfactory. The accuracy rate of abdominal CE-CT imaging for the T factor was identical to that of PET/CE-CT imaging, since the CE-CT portion is the main evaluation tool for T factor analysis even on PET/CE-CT

imaging. With respect to the N factor, Higashi et al. [16] reported that the diagnostic accuracy rate assessed by CT images was not satisfactory. Zimny et al. [17] reported a low accuracy rate for FDG-PET in evaluation of the N factor as well. In the present study, the diagnostic accuracy rate of PET/CE-CT for the N factor was 42%, despite the fact that the diagnosis was based on both CT images of the size and shape of lymph nodes and FDG uptake on PET, while the diagnostic accuracy rate of abdominal CE-CT was even lower (35%). The extent of the N factor was differentially diagnosed with PET/CE-CT and histological examination in 18 cases; however, of these 18 cases, 9 cases of Group 1-lymph node metastasis were diagnosed as N0 on PET/CE-CT but as N1 by histological examination. These lymph nodes were attached to the resected specimens; therefore, detection of such lymph node metastasis by imaging seems impossible because of their small size and/or their merging with pancreatic tumors. If these 9 cases were excluded from our calculation of the diagnostic accuracy rate, the accuracy rate of PET/CE-CT for the N factor would be 13/22 (59%), although even this level is low. These results indicate that PET/CE-CT imaging is not very useful for assessing the N factor, which is consistent with previous reports [16, 17]. On the other hand, PET/CE-CT is very useful in evaluation of the M factor, as indicated by the high accuracy rate of PET/CE-CT within this context. In fact, the diagnostic accuracy rate of PET/CE-CT for the M factor was 94% in 31 patients with stage IVa resectable cancers. Furthermore, in 65 patients with stage IVb unresectable cancers, the detection rates of PET/CE-CT for metastases to the lymph nodes (N3), liver, peritoneum, lung, and bone were 51%, 55%, 53%, 18%, and 24%, respectively. These detection rates for distant lymph node (N3) and peritoneum metastases were significantly higher for PET/CE-CT imaging than for abdominal CE-CT imaging. The detection rates of PET/CE-CT for lung and bone metastases were also higher than those of abdominal CE-CT imaging. However, such differences

were attributed to the nature of PET/CE-CT scans (whole body imaging) and abdominal CE-CT scans (imaging of only a segmental area). Therefore, in the pre-operative evaluation of the extent of pancreatic cancer, which is important for deciding treatment options, our present results suggest that PET/CE-CT is a useful tool for assessing T and M factors, but is not very useful for assessing the N factor. This is consistent with a report by Strobel et al. [18], in which PET/CE-CT was found to be superior to PET imaging alone in assessing the respectability of pancreatic cancer.

When PET was first developed, many published reports stated that the SUV_{max} could be useful for differentially diagnosing malignancies and benignancies [16, 19]. Nishiyama et al. [20] and Nakamoto et al. [21] reported that a malignancy could be differentiated from a benignancy in pancreatic disorders based on the SUV_{max} to delayed scan ratio. However, as described in the present study, the SUV_{max} of malignant pancreatic tumors overlapped with that of benign pancreatic diseases, suggesting that distinguishing between benign and malignant cases through SUV_{max}-based diagnosis is difficult. Extremely high SUV_{max} values were observed in 2 cases of benign pancreatic endocrine tumor in the present study. The SUV_{max} varies according to the several factors, including blood glucose levels, Glut 1 expression, glucose-6-phosphatase expression, and tumor heterogeneity, etc. [16]. In a previous study, high SUV_{max} values were found in tumors with high Glut 1 expression [22]. In our study, extremely high SUV_{max} values were observed in 2 cases of benign endocrine tumors, and these high values may be attributed to high Glut 1 expression in these tumors; however, Glut 1 expression was not examined histologically. In order to differentiate between benignancy and malignancy of pancreatic tumor lesions by PET/CE-CT imaging, we first assessed the invasion of the tumors into surrounding organs/vessels and other malignancy-indicating signs by analysis of the CE-CT portion of

PET/CE-CT imaging and then diagnosed the case by referring to the FDG uptake data (SUV_{max}) by analysis of the PET portion. We did not use SUV_{max} values for differentiating between benignancy and malignancy. So, what is the meaning of SUV_{max} in the clinical management of pancreatic cancer? In the present study, we examined correlations between the SUV_{max}, tumor size, and tumor marker (CA19-9) levels in unresectable locally advanced pancreatic cancer under treatment. During the course of treatment, SUV_{max} and CA19-9 levels showed substantial positive correlations in the change rate, while SUV_{max} and tumor size showed significant, although slight, positive correlations. However, no significant correlation was found between tumor marker levels and tumor size. Treatment effects on solid tumors were assessed by determining tumor size by imaging according to the RECIST criteria [12] and by the levels of serum tumor markers. In pancreatic cancer, however, changes in tumor size do not necessarily reflect treatment effects, since pancreatic cancers contain a variety of interstitial components. Thus, we have frequently experienced discrepancies between changes in tumor size and tumor marker levels in assessing the effects of treatment, which makes it difficult to determine the effects of treatment in these cases. Identification of an additional indicator would help in determining the effects of treatment on pancreatic cancer progression/regression. In the present study, we demonstrated that the SUV_{max} measured by PET proved useful in this regard. Similarly, Yoshioka et al. [23] reported that the SUV_{max} was useful to monitor the effects of treatment on pancreatic cancers. These findings, together with those in the present study, suggest that the SUV_{max} is a useful indicator for the effects of treatment on pancreatic cancer. The addition of the SUV_{max} to the existing indicators (tumor size and markers) is expected to reduce the difficulty of assessing the effects of treatment on pancreatic cancer progression.

Since either invasion into the surrounding regions or distant metastasis is often already involved

at the time of pancreatic cancer diagnosis, less than 20% of cases are treated surgically [24]. Even when surgery is employed, recurrence usually occurs very soon thereafter [13]. Therefore, cautious observation is required after surgery. In general, abdominal CE-CT is conducted every 3–6 months for postoperative monitoring. Local, hepatic, and peritoneal recurrences are frequently observed postoperatively. Abdominal CE-CT can be used to diagnose hepatic recurrence, but it is sometimes difficult to detect local or peritoneal recurrences due to postoperative changes in the anatomical positions of organs [15, 17]. Ruf et al. [25] showed that FDG-PET is superior to CT/MRI in the detection of local recurrences of pancreatic cancers. In the present study, we demonstrated that the diagnostic accuracy of PET/CE-CT is superior to abdominal CE-CT in predicting the postoperative local recurrence of pancreatic cancer. Considering the postoperative changes in the anatomical positions of abdominal organs, PET/CE-CT imaging, which employs both contrast-enhanced CT and PET functions, is recommended for postoperative monitoring.

Conclusion

In the present study, we demonstrated that PET/CE-CT imaging can provide useful information in the clinical management of pancreatic cancer. We recommend PET/CE-CT imaging as the first choice examination for suspected pancreatic cancer, staging, assessment of treatment effectiveness, and confirmation of suspected recurrence.

Conflict of Interest

The authors declare that they have no potential conflicts of interest.

References

1. Jemal A, Siegel R, Xu J, et al. Cancer statistics, 2010. CA Cancer J Clin. 2010;60:277-300.

2. Matsuda T, Marugame T, Kamo K, et al. Cancer incidence and incidence rates in Japan in 2003: based on data from 13 population-based cancer registries in the Monitoring of Cancer Incidence in Japan (MCIJ) Project. Jpn J Clin Oncol. 2009;39:850-858.

3. Burris HA, 3rd, Moore MJ, Andersen J, et al. Improvements in survival and clinical benefit with gemcitabine as first-line therapy for patients with advanced pancreas cancer: a randomized trial. J Clin Oncol. 1997;15:2403-2413.

4. Okusaka T, Funakoshi A, Furuse J, et al. A late phase II study of S-1 for metastatic pancreatic cancer. Cancer Chemother Pharmacol. 2008;61:615-621.

5. Smith SL, Rajan PS. Imaging of pancreatic adenocarcinoma with emphasis on multidetector CT. Clin Radiol. 2004;59:26-38.

6. Ell PJ. The contribution of PET/CT to improved patient management. Br J Radiol. 2006;79:32-36.

7. Reinartz P, Wieres FJ, Schneider W, et al. Side-by-side reading of PET and CT scans in oncology: which patients might profit from integrated PET/CT? Eur J Nucl Med Mol Imaging. 2004;31:1456-1461.

8. Isaji S, Kawarada Y, Uemoto S. Classification of pancreatic cancer: comparison of Japanese and UICC classifications. Pancreas. 2004;28:231-234.

9. Otsuki M. Chronic pancreatitis in Japan: epidemiology, prognosis, diagnostic criteria, and future problems. J Gastroenterol. 2003;38:315-326.

10. Okazaki K, Kawa S, Kamisawa T, et al. Clinical diagnostic criteria of autoimmune pancreatitis: revised proposal. J Gastroenterol. 2006;41:626-631.

11. DeLellis RA LR, Heitz PV, Eng C. Pathology and Genetics Tumor of Endocrine Organs (World Health Organization Classification of Tumors). IARC Press, 2004.

12. Therasse P, Arbuck SG, Eisenhauer EA, et al. New guidelines to evaluate the response to treatment in solid tumors. European Organization for Research and Treatment of Cancer, National Cancer Institute of the United States, National Cancer Institute of Canada. J Natl Cancer Inst. 2000;92:205-216.

13. Geer RJ, Brennan MF. Prognostic indicators for survival after resection of pancreatic adenocarcinoma. Am J Surg. 1993;165:68-72.

14. Goldberg RM, Fleming TR, Tangen CM, et al. Surgery for recurrent colon cancer: strategies for identifying resectable recurrence and success rates after resection. Eastern Cooperative Oncology Group, the North Central Cancer Treatment Group, and the Southwest Oncology Group. Ann Intern Med. 1998;129:27-35.

15. Barkin JS, Goldstein JA. Diagnostic approach to pancreatic cancer. Gastroenterol Clin North Am. 1999;28:709-722.

16. Higashi T, Saga T, Nakamoto Y, et al. Diagnosis of pancreatic cancer using fluorine-18 fluorodeoxyglucose positron emission tomography (FDG PET) --usefulness and limitations in "clinical reality". Ann Nucl Med. 2003;17:261-279.

17. Zimny M, Bares R, Fass J, et al. Fluorine-18 fluorodeoxyglucose positron emission tomography in the differential diagnosis of pancreatic carcinoma: a report of 106 cases. Eur J Nucl Med. 1997;24:678-682.

18. Strobel K, Heinrich S, Bhure U, et al. Contrast-enhanced 18F-FDG PET/CT: 1-stop-shop imaging for assessing the resectability of pancreatic cancer. J Nucl Med. 2008;49:1408-1413.

19. Delbeke D, Rose DM, Chapman WC, et al. Optimal interpretation of FDG PET in the diagnosis,

staging and management of pancreatic carcinoma. J Nucl Med. 1999;40:1784-1791.

20. Nishiyama Y, Yamamoto Y, Monden T, et al. Evaluation of delayed additional FDG PET imaging in patients with pancreatic tumour. Nucl Med Commun. 2005;26:895-901.

21. Nakamoto Y, Higashi T, Sakahara H, et al. Delayed (18)F-fluoro-2-deoxy-D-glucose positron emission tomography scan for differentiation between malignant and benign lesions in the pancreas. Cancer. 2000;89:2547-2554.

22. Higashi T, Tamaki N, Honda T, et al. Expression of glucose transporters in human pancreatic tumors compared with increased FDG accumulation in PET study. J Nucl Med. 1997;38:1337-1344.

23. Yoshioka M, Sato T, Furuya T, et al. Role of positron emission tomography with 2-deoxy-2-[18F]fluoro-D-glucose in evaluating the effects of arterial infusion chemotherapy and radiotherapy on pancreatic cancer. J Gastroenterol. 2004;39:50-55.

24. Wray CJ, Ahmad SA, Matthews JB, et al. Surgery for pancreatic cancer: recent controversies and current practice. Gastroenterology. 2005;128:1626-1641.

25. Ruf J, Lopez Hanninen E, Oettle H, et al. Detection of recurrent pancreatic cancer: comparison of FDG-PET with CT/MRI. Pancreatology. 2005;5:266-272.

Figure Legends

Figure 1: Stage grouping of pancreatic cancers according to JPS guidelines [8].

Stages of pancreatic cancer are grouped into 5 categories according to the cancer extent based on the grading of T, N, and M factors.

Figure 2: SUV_{max} of different pancreatic tumor lesions.

Ninety minutes after FDG infusion in various pancreatic tumor cases, PET/CE-CT scans were conducted to determine the SUV_{max}. Patients with blood glucose levels of 200 mg/dL or less at the time of FDG infusion were evaluated.

Figure 3: PET/CE-CT findings of a typical case (86-year old woman) with lymph node metastasis.

The CE-CT image shows #16b1 lymph node swelling (10.5 × 5.0 mm, flat shape); however, lymph node metastasis was ruled out based on the size and shape of the swelling as determined by CT (A). The PET/CT image, on the other hand, shows abnormal FDG uptake (SUV_{max}, 2.61) corresponding to this lymph node (B), suggesting lymph node metastasis. Histological examination of the surgical specimen proved the involvement of lymph node lesions.

Figure 4: Monitoring treatment effectiveness in invasive pancreatic ductal cancer by PET/CE-CT.

Chemotherapy or chemoradiotherapy was conducted in 8 patients with unresectable locally advanced pancreatic cancer. PET/CE-CT imaging (SUV_{max} by PET and tumor size by CE-CT) and levels of serum tumor markers (CA19-9) were used to assess the effects of treatment over time. Only tumors that were found to be locally confined during treatment were analyzed. Cases in which distant metastasis occurred were excluded from analysis.

A. Changes in tumor size, CA19-9, and SUV_{max} during treatment.

Compared to the baseline values (100%), the values at PR or PD are indicated by the % decrease or increase.

B. Correlations between the rate of change in tumor size, CA19-9, and SUV_{max} during treatment. (NS: not significant)

Figure 5: PET/CE-CT findings of 2 typical cases, 1 with “local recurrence” and the other with “no local recurrence,” are shown.

A. A 46-year-old man with no local recurrence (false-positive by CE-CT and true-negative by PET/CE-CT).

The CE-CT image, which was performed 17 months after surgery, showed a soft-tissue density mass, which did not rule out local recurrence (left upper panel, arrow). However, the PET/CT image did not show FDG uptake corresponding to this mass, suggesting no

local recurrence (left lower panel, arrow). A follow-up PET/CE-CT image, which was performed 8 months after the initial examination, revealed no increase in the size and FDG uptake of the mass (right panel, arrow), indicating that the initial diagnosis of no local recurrence by PET/CE-CT was correct.

B. A 59-year-old man with local recurrence (true-positive by CE-CT and PET/CE-CT).

The CE-CT image, which was performed 3 months after surgery, showed a soft-tissue density mass, which did not rule out local recurrence (left upper panel, arrow). The PET/CT image shows abnormal FDG uptake (SUV_{max}, 4.73) corresponding to this mass, suggesting local recurrence (left lower panel, arrow). A follow-up PET/CE-CT image, which was performed 3 months after the initial examination, revealed an increase in the size and FDG uptake (SUV_{max}, 6.99) of the mass (right panel, arrow), indicating that the initial diagnosis of local recurrence by PET/CE-CT was correct.

Table 1:

A.

	PET/CE-CT
T factor: Ts	14/28 (50%)
CH	24/29 (83%)
DU	26/29 (90%)
S	22/29 (76%)
RP	19/29 (66%)
PV	25/29 (86%)
A	28/29 (97%)
PL	24/29 (83%)
OO	29/29 (100%)
N factor:	13/31 (42%)
M factor:	29/31 (94%)

B.

Extent of N factor		Number of cases
PET/CT imaging	histological examination	(n=18)
N3, N2	→ N1	4
N1	→ N0	2
N0	→ N1	9
N0	→ N2	1
N0	→ N3	2

A: Diagnostic accuracy rate of PET/CE-CT imaging in determining the extent of cancer in 31 patients with pre-operative stage IVa resectable pancreatic cancer.

The extent of cancer was determined with regard to local spread (T), lymph node metastasis (N), and distant metastasis (M) according to the classification guidelines for pancreatic carcinomas published by the Japan Pancreas Society (8). Pre-operative cancer extent diagnosed by PET/CE-CT imaging and histological examination of resected specimens were compared among 29 patients with stage IVa resectable pancreatic cancer to calculate the diagnostic accuracy rate of PET/CE-CT imaging. Ts was not assessable in 1 resected specimen; therefore, Ts was determined in 28 specimens. Distant metastases were histologically proven in 4 more cases (2 lymph node [N3], 1 hepatic, and 1 peritoneal metastasis), in addition to 29 patients with stage IVa resectable pancreatic cancer, in whom only tissue biopsies were performed after initiation of the surgical procedure. These 4 cases were included in N and M factor evaluation; therefore, N and M factors were histologically determined in 31 specimens.

Ts, tumor size; CH, distal bile duct; DU, duodenum; S, serosa; RP, retropancreatic tissue; PV, portal vein system; A, arterial system; PL, extrapancreatic nerve plexus; OO, other organ.

B: Breakdown of the differently diagnosed extent of the N factor with PET/CE-CT imaging and histological examination in 18 of 31 patients with pre-operative stage IVa resectable pancreatic cancer.

Table 2: Difference between PET/CE-CT and abdonimal CE-CT in the diagnosis of the extent of M factor progression in 65 patients with stage IVb unresectable pancreatic cancer.

	PET/CE-CT	abdominal CE-CT
Lymph node (N_3)	33 (51%)	29 (45%) †
Liver	36 (55%)	35 (53%)
Peritoneum	35 (53%)	20 (31%) ‡
Lung	12 (18%)	5 (8%) ‡
Bone	16 (24%)	3 (5%) ‡

PET/CE-CT was conducted at the time of diagnosis in 65 patients. The portions that correspond to the abdominal CE-CT were extracted from the PET/CE-CT images and reconstructed. Then, 2 radiologists assessed the extent of M factor characteristics on these extracted images. If a disagreement occurred, a final decision was made after discussion between the radiologists.

† $p < 0.05$ vs. PET/CE-CT
‡ $p < 0.01$ vs. PET/CE-CT

Table 3: PET/CE-CT vs. abdominal CE-CT for the diagnosis of postoperative local recurrence.

		PET/CT	
		recurrence (n = 11)	no recurrence (n = 6)
CT	recurrence	7	1
	No recurrence	4	5
	Accuracy rate	63%	83%

Above are 11 cases diagnosed as “local recurrence” and 6 cases diagnosed as “no recurrence” by PET/CE-CT imaging during the postoperative monitoring period. The portion that corresponds to the abdominal CE-CT was extracted from PET/CE-CT images and reconstructed. Local recurrence was diagnosed by PET/CE-CT based on the findings of soft tissue-density mass with FDG accumulation, while soft tissue-density mass without FDG accumulation was diagnosed as a postoperative change. The diagnosis of local recurrence by abdominal CE-CT, on the other hand, required not only the presence of soft tissue-density mass, but also the comparison of the current tumor size with the previous measure of tumor size. Two radiologists assessed local recurrence on these extracted images. If a disagreement occurred, a final decision was made after discussion between the radiologists.

Fig. 1

<table>
<tr><td rowspan="2"></td><td colspan="3">M0</td><td colspan="2">M1</td></tr>
<tr><td>N0</td><td>N1</td><td>N2</td><td>N3</td></tr>
<tr><td>T1</td><td>Ⅰ</td><td>Ⅱ</td><td>Ⅲ</td><td colspan="2" rowspan="4">Ⅳb</td></tr>
<tr><td>T2</td><td>Ⅱ</td><td>Ⅲ</td><td>Ⅲ</td></tr>
<tr><td>T3</td><td>Ⅲ</td><td>Ⅲ</td><td>Ⅳa</td></tr>
<tr><td>T4</td><td colspan="3">Ⅳa</td></tr>
</table>

Fig. 2

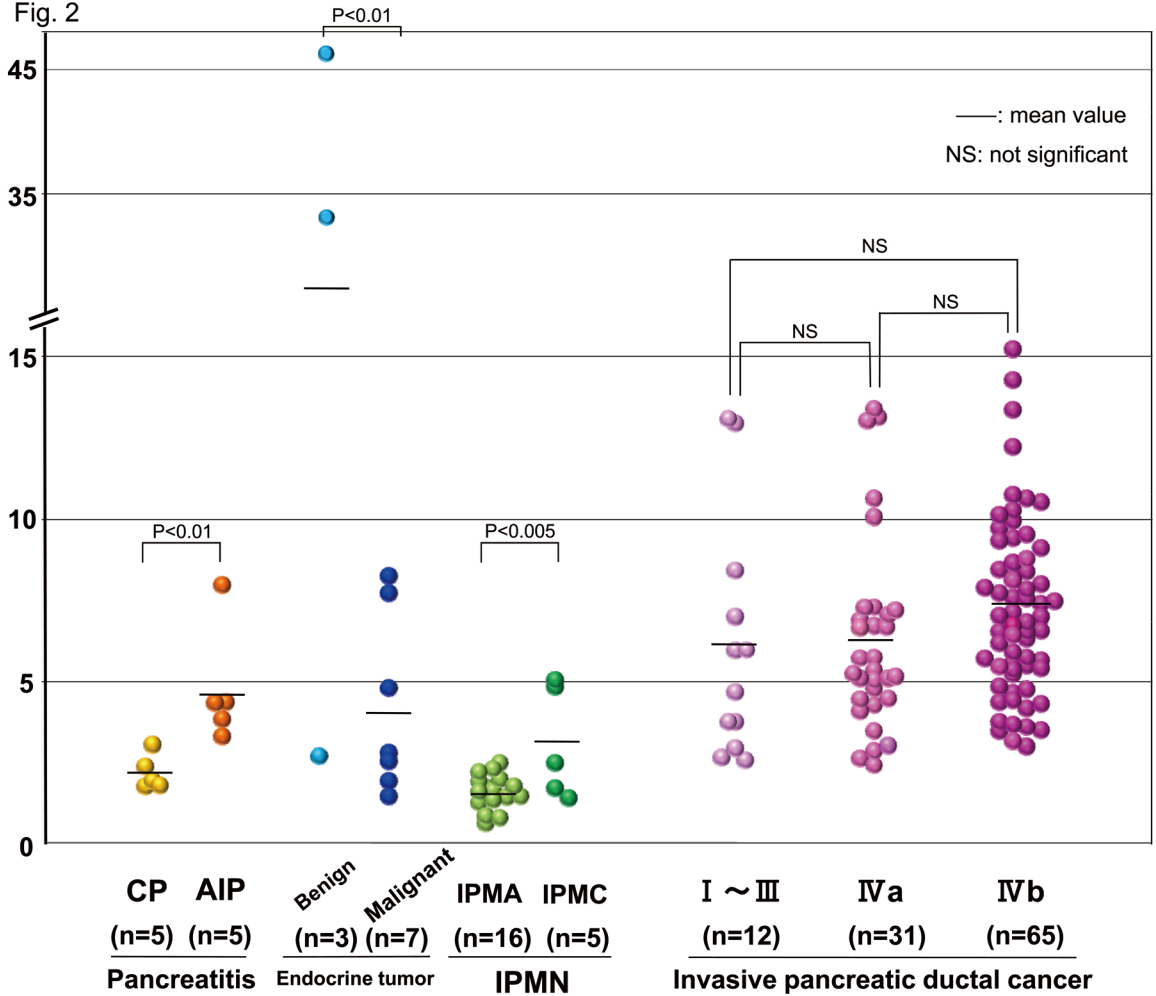
P<0.01
45
35
15
10
5
0
——: mean value
NS: not significant
NS
NS
NS
P<0.01
P<0.005
CP
AIP
Benign
Malignant
IPMA
IPMC
Ⅰ～Ⅲ
Ⅳa
Ⅳb
(n=5)
(n=5)
(n=3)
(n=7)
(n=16)
(n=5)
(n=12)
(n=31)
(n=65)
Pancreatitis
Endocrine tumor
IPMN
Invasive pancreatic ductal cancer

Fig. 3

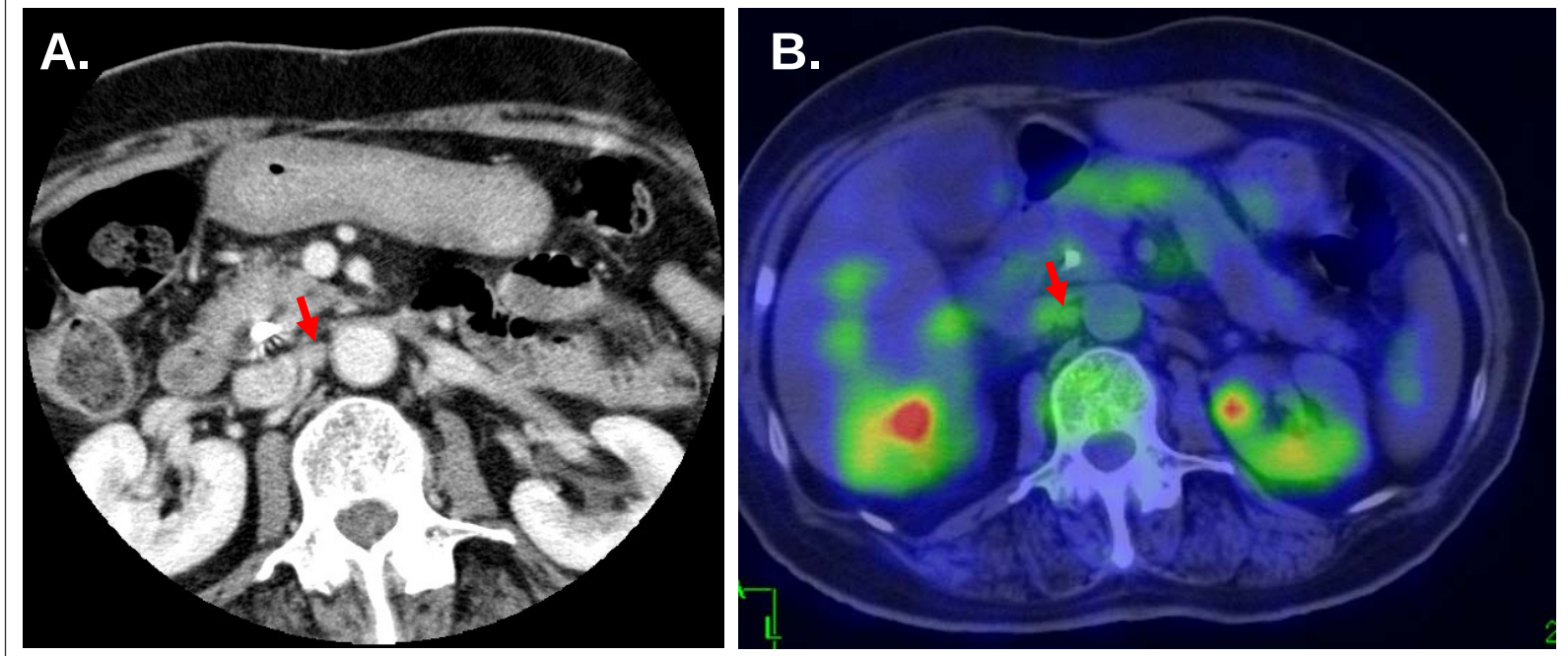

Fig. 4

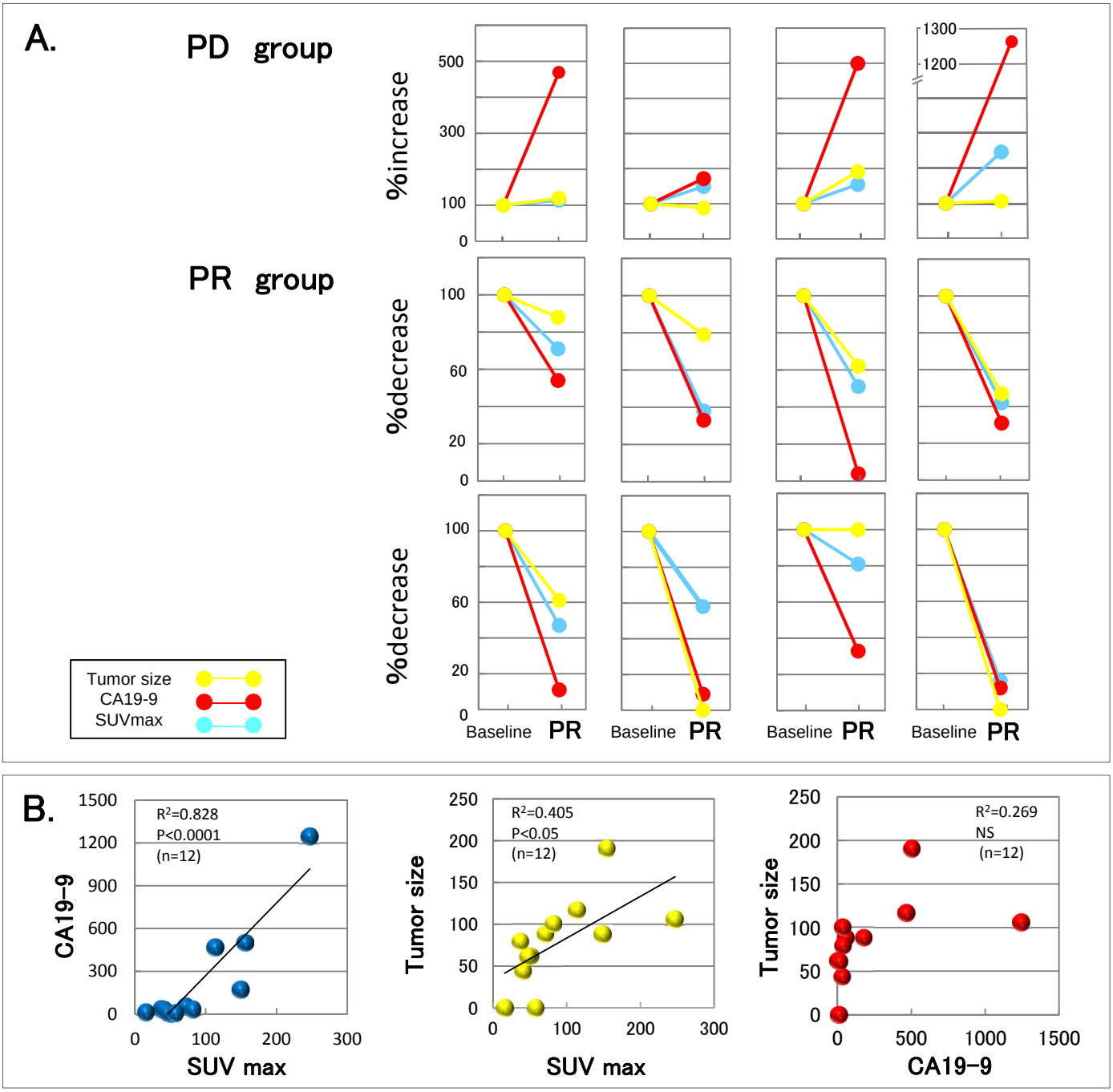
A.
PD group
PR group
%increase
%decrease
%decrease
500
300
100
0
1300
1200
100
60
20
0
Baseline
PR
Tumor size
CA19-9
SUVmax
B.
R²=0.828
P<0.0001
(n=12)
CA19-9
SUV max
1500
1200
900
600
300
0
100
200
300
R²=0.405
P<0.05
(n=12)
Tumor size
SUV max
250
200
150
50
R²=0.269
NS
(n=12)
Tumor size
CA19-9
500
1000
1500

Fig. 5